MUSCULOSKELETAL

Stefan Hinterwimmer
Heiko Graichen
Thomas J. Vogl
Nasreddin Abolmaali

# An MRI-based technique for assessment of lower extremity deformities—reproducibility, accuracy, and clinical application

S. Hinterwimmer · H. Graichen
Research Group for Kinematics
and Biomechanics,
Department of Orthopedic Surgery,
University of Frankfurt,
Marienburgstr. 2,
60528 Frankfurt, Germany

S. Hinterwimmer
Department of Orthopaedic Sports
Medicine, Klinikum Rechts der Isar,
Technische Universität München,
Connollystr. 32,
80809 München, Germany

H. Graichen
Asklepios Clinic for Orthopedics and
Traumatology Lindenlohe,
Lindenlohe 18,
92421 Schwandorf, Germany

T. J. Vogl · N. Abolmaali
Institute of Diagnostic and
Interventional Radiology,
JW Goethe University of Frankfurt,
Theodor Stern Kai 7,
60590 Frankfurt, Germany

N. Abolmaali (✉)
OncoRay - Molecular Imaging,
Medical Faculty Carl Gustav Carus,
TU Dresden,
Fetscherstraße 74, PF 86,
01307 Dresden, Germany
e-mail: Nasreddin.Abolmaali@
OncoRay.de
Tel.: +49-351-4587414
Fax: +49-351-449210394

**Abstract** The hypothesis of this study was that length, torsion, and axis of a leg phantom can be measured accurately and reproducibly by magnetic resonance imaging (MRI) and that this can be applied to patients with leg deformities. Two phantoms and 30 patients (genu varum, $n=15$; genu valgum, $n=15$) were investigated using an optimized MRI technique. Reference measurements were performed with a micrometer screw and a goniometer. Patient leg length and axis were compared with long radiographs in bipedal stance. Intra- and inter-observer reproducibility and accuracy were calculated using the mean absolute difference (MAD) and the 95% confidence interval. In patients, comparisons were done using a paired Student's $t$-test. MAD, intraobserver MAD, and interobserver MAD were 0.03, 0.03, 0.04 mm (length); 0.98, 1.2, 0.98° (torsion); and 0.18, 0.23, 0.22° (axis), respectively. In patients, leg length was underestimated by MRI ($-2.4\pm0.7\%$; $1.9\pm0.7$ cm; $P<0.001$). The hip-knee-ankle angle (HKA) did not show significant differences in varus knees ($-0.5\pm1.0°$; $P>0.05$), while it was significantly underestimated in valgus knees ($-3.6\pm2.8°$; $P<0.05$). The phantom study revealed that leg length, torsion, and axis can be measured accurately and reproducibly by MRI. Although underestimation of leg length and HKA in valgus knees occurred, this optimized MRI technique can be applied to patients with leg deformities.

**Keywords** Magnetic resonance · Comparative study · Bone measurement · Phantom · Spatial distortion correction

## Introduction

Exact geometrical analysis of lower-limb deformities is essential prior to surgical correction [1, 2]. Long radiographs with the patient standing in bipedal stance in the frontal and lateral projection are regarded to be the standard of reference [3]. Additionally, computed tomography (CT) and ultrasound examinations can quantify both leg length discrepancies and the torsion of femur and tibia [4–6]. Long radiographs and CT are burdened by radiation exposure [7]. Ultrasound, on the other hand, shows only limited accuracy [5, 8].

After complications of femoral and tibial fractures, length discrepancies are often combined with torsion and axis deformities [9]. Here long radiographs together must be used in combination with CT and/or ultrasound, both

for preoperative planning but even more for postoperative control, increasing the risks delivered by radiation exposure.

Magnetic resonance imaging (MRI) can definitely solve the problem of radiation exposure. However, it has not yet been established for preoperative planning of corrective surgery, even though first experiences in the comparison of radiography, CT, and MRI on cadaveric femurs have been published [10]. Currently, MRI is part of the diagnostic procedure only in pediatric patients with femoral anteversion prior to rotation osteotomies [11] and growth-plate changes in tibia vara prior to oblique osteotomy or tibial hemiepiphysiodesis [12]. The technical limitations are that the field of view (FoV) of typical clinical scanners does not allow imaging of objects larger than 50 cm without table movement and that conventional high-field (> 1 Tesla) MRI systems cannot simulate the effect of full weight bearing on the limb axis because of the supine imaging position. Additionally, geometrical distortions that increase nonlinearly towards the margins of the FoV hamper the measurement accuracy. Therefore, length measurement errors in particular can be expected if the FoV is larger than 250–300 mm.

To improve the visualization of cortical bone for length and angle measurements, the thickness of the corticalis should be depicted properly. Therefore, chemical shift artifacts altering the thickness of the corticalis by the lipids in the bone marrow should be reduced by selecting a high bandwidth. Furthermore, the sensitivity of the selected sequence technique to susceptibility artifacts should be as low as possible to further minimize geometrical distortions. The legs should be placed on the scanner table in a way that all bones of the lower extremity are positioned horizontally to avoid artificial shortening of the legs by an oblique course of the bones through the imaging plane. It is important to acquire the entire data in a short period of time to reduce the possibility that patient movements occur during image acquisition. To some extent, this precludes the application of MRI surface coils along the entire lower extremities, since patient positioning should be done quickly as well. The contrast weighting of the sequence should particularly provide anatomical information; the visualization of edema or other pathological changes is not required.

The aim of this study was to develop and apply a uniform radiation-free measurement technique for the analysis of leg geometry. Therefore, reproducibility and accuracy of an optimized MRI technique was validated using standard table movement methods in a phantom study. Subsequently, we applied this technique to patients with varus and valgus knees measuring leg length and axis each compared to long radiographs. The specific questions to be answered were as follows:

1. How reproducible and accurate is the new MRI technique for determination of length, torsion, and axis when analyzing geometrically defined phantoms?

2. Is there a difference between the MRI technique (supine position) and long radiographs (bipedal stance) in the analysis of leg length and alignment in patients with varus and valgus deformity?

## Methods

### MR imaging

All examinations were performed with a 1.5-T closed MRI system (Magnetom Sonata, Siemens, Erlangen, Germany) with the body coil, i.e., without surface coils. A turbo-spin echo (TSE) sequence was used for image acquisition rather than an SE sequence, since the inherent sensitivity to susceptibility artifacts is lower and the acquisition time is shorter. The bandwidth was set to 500 Hz/pixel to reduce chemical shift artifacts that could impair length and angle measurements of bony structures. Furthermore, this allowed minimizing TE (echo time) and TR (repetition time) to 4.4 ms and 872 ms, respectively, to increase image acquisition speed. Slice thickness (SL) was 8 mm, in-plane resolution using a $128 \times 256$ matrix was $1.56 \times 1.56$ mm. Using a head-to-feet phase encoding direction, the FoV was set to 400 mm in the frequency encoding direction and reduced to 200 mm in the phase encoding direction to reduce gradient field-related image distortions at the borders of the images. Utilizing 100% phase oversampling avoided wraparound artifacts. The true coronal slabs consisted of 20 images each, covering 175.2 mm (gap 10%) in the slice encoding direction. By incremental and automated table repositioning, five consecutive imaging positions without overlap or gap were acquired from the hip joint downwards until the ankle was depicted. The parameters were selected to facilitate an adequate signal-to-noise ratio together with short data acquisition. The imaging time for five leg positions covering 100 cm was 2:05 min.

Adjusted at the coronal images, additional axial images were acquired along the femoral head and neck, the knee, and the ankle, applying the same sequence with individually reduced phase oversampling to facilitate torsion measurements of the femur and tibia [6].

With this, the imaging time in total was approximately 4–5 min; adequate patient positioning required an additional 2 min.

### Phantom study

To verify MRI-based length measurements, a custom-built phantom (phantom 1) made of acrylic glass (dimensions: $2 \times 2 \times 100$ cm) with drill holes of exactly 1 cm depth and 0.4 cm diameter was investigated (Fig. 1). The drill holes were placed along an exactly straight line at intervals of 5 cm. The precision of the phantom measures was 0.1 mm.
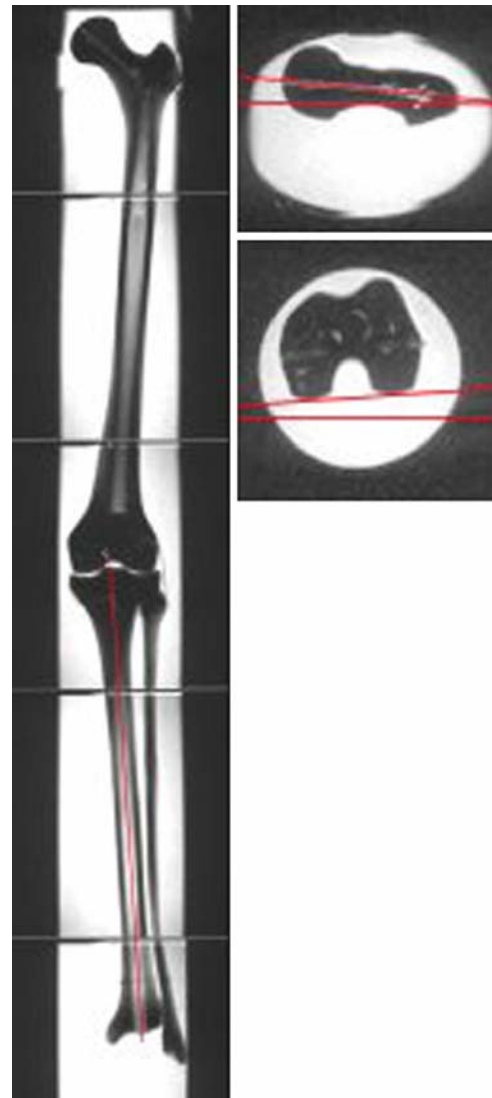
**Fig. 1** MR image of an acrylic glass phantom with drill holes placed along an exactly straight line at intervals of 5 cm
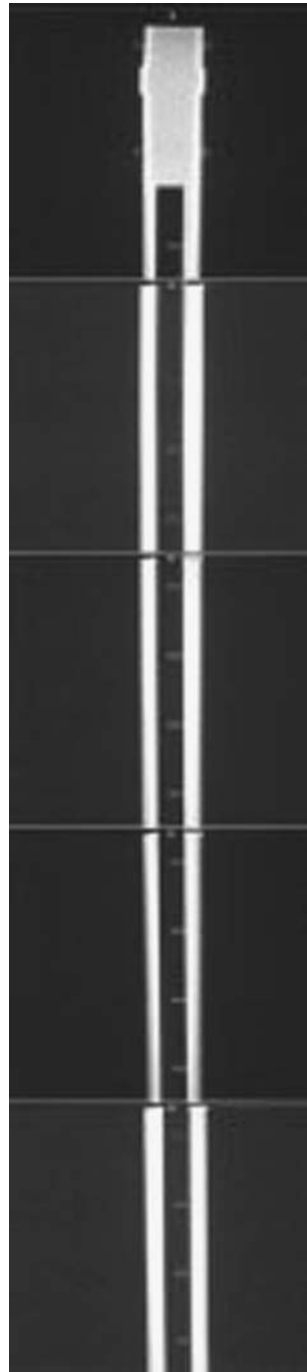
diluted contrast agent (Gd-DTPA, 1:200). Thus the phantoms appeared as a negative in their contrast-agent bed (Figs. 1, 2 and 3), and the drill holes of the acrylic glass phantom were filled with contrast agent (Fig. 1). The plastic tube containing the phantoms was placed horizontally into the MR system, and image acquisition was done as mentioned above.

Patient study

We examined the legs of 30 patients (mean age 61.7± 15.2 years, median 62 years, range 30–83 years) suffering



**Fig. 2** MR image of a plastic bone phantom with femur and tibia in supine position. *Red lines* indicate torsion of the femur (axial images) and anatomical axis of the tibia (coronal image)

To verify MRI-based torsion and axis measurements, a plastic leg phantom (femur and tibia, phantom 2) (Sawbones Europe AB, Malmö, Sweden) was investigated, first in its original status (Fig. 2), then after femur osteotomy with 20° external torsion deformity (original torsion = 8° anteversion, leading to 28° external torsion) and tibia osteotomy with 20° varus deformity (Fig. 3). The phantoms were bedded in an air-free plastic tube filled with
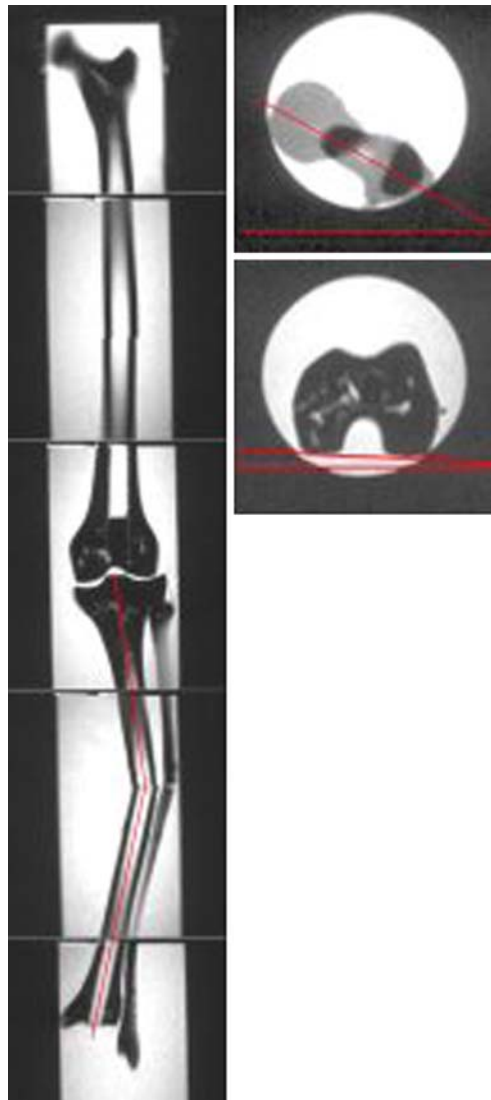
**Fig. 3** MR image of a plastic bone phantom after torsion osteotomy (20°) of the femur and closed wedge varus osteotomy (20°) of the tibia. *Red lines* indicate torsion of the femur (axial images) and anatomical axis of the tibia (coronal image)

from osteoarthritis (OA) with genu varum (*n*=15) (Fig. 4) and genu valgum (*n*=15) (Fig. 5) prior to proximal tibial osteotomy or implantation of total knee endoprosthesis. Both surgeries were performed after diagnosis and planning with scaled long radiographs and the patient standing in bipedal stance with load on both legs (patella orientation in front, beam centered on the affected knee joint, film-to-focus distance of 250 cm, estimated distance of the femoral head to the film: 15 cm, from the ankle joint to the film: 5 cm). The images were taken on a digital film (minimum film size 40×120 cm). X-ray examination was performed 1 day prior to surgery.

Additionally, all patients were examined by MRI on the same day as x-ray was performed. Patients were investigated in a supine position with hip and knee straight and ankle in neutral position using several different pads to acquire the images of thigh, shank, and joints of the lower extremity in matching imaging planes and without artificial shortening. The thickness of the pads increased from knee to ankle to facilitate true coronal images without angulation along the femur. The legs of the patients and the pads were fixed to the table with several straps to exclude patient movement during the image acquisition. Image acquisition was done as mentioned above. Out of each slab one image for each leg was selected as follows. At the hip joint, the image displaying the uppermost part of the femoral head was selected. From the second slab, the image with the most complete visualization of the thigh was chosen. At the



**Fig. 4** Long radiograph versus MR image in a varus knee. *Red lines* indicate hip-knee-ankle angle showing only slight differences between both techniques

**Fig. 5** Long radiograph versus MR image in a valgus knee. *Red lines* indicate hip-knee-ankle angle showing significant differences between both techniques

knee, the image displaying the tubercles of the intercondylar eminence was selected. From the fourth slab, the image with the most complete visualization of the shank was chosen. At the ankle, the image displaying the position of maximum convexity of the distal tibia pointing toward the center of the talar dome was selected. These five images were sent to a laser imager (Figs. 4 and 5).

All participants received oral and written information regarding the nature of the examination and the study and signed a statement of informed consent that had been approved by the local Ethics Committee.

Data analysis

After scaled import of radiographs and MR images, all data analysis was done digitally on the laser images or on the monitor. In the phantom, length was measured as the distance from the middle of the most proximal to the middle of the most distal drill hole. The femoral torsion angle was measured as the angle between the head-neck centerline and the posterior condylar plane [13]. The anatomical axis of the tibia was defined as the longitudinal axis of the shaft [14]. In the patients, leg length was determined by measuring the distance from the tip of the head of femur to the center of the distal tibial articular surface [4]. The HKA angle was defined as the angle between the mechanical axis of femur and tibia [15].

To test the intra- and interobserver reproducibility of the MRI technique, length (phantom 1), torsion (phantom 2, femur) and axis measurements (phantom 2, tibia) were performed by three independent investigators, (S.H., H.G., N.A.) six times each. The mean absolute differences (MAD) [16–18] and the 95% confidence intervals (95% CI) within and between examiners were calculated. For intraobserver reproducibility, statistical significance was tested by a one-sample *t*-test.

The accuracy of the measurements was assessed by calculating MAD and 95% CI for the values obtained from MR imaging compared with the real length of the entire acrylic glass phantom and the real femur torsion and tibia alignment of the bone phantom determined by physical measurement with micrometer screw and goniometer, respectively.

For clinical application, the differences in HKA angle measurement and leg length measurement between long radiographs and the MRI technique were tested for statistical significance using a paired Student's *t*-test.

All caliper measurements were done by each investigator separately on different days using anonymized images in a random order. Data were registered by a fourth person without revealing the former values. With all of this, a "memory effect" of the investigators should be limited.

## Results

Phantom study

Regarding the reproducibility of the MRI measurement, the maximum intraobserver MADs were 0.03 mm for the length, 1.2° for torsion and 0.23° for axis measurement (Table 1). The equivalent values for interobserver reproducibility were 0.04 mm for length, 1.31° for torsion and 0.22° for axis measurement (Table 2).

The accuracy of the MRI measurement was again expressed by the MAD, in this case between the MRI and the physical measurement of the phantoms with micrometer screw and goniometer (Table 3). The MAD

**Table 1** Intraobserver reproducibility of length analysis of the acrylic glass phantom (phantom 1), torsion analysis of the femur phantom (phantom 2), and anatomical axis analysis of the tibia phantom (phantom 2)

|  | MAD | 95% CI | $P^a$ |
|---|---|---|---|
| **Length (mm)** |  |  |  |
| Observer 1 | 0.02 | −0.04 to 0.10 | 0.4 |
| Observer 2 | 0.03 | −0.07 to 0.13 | 1.0 |
| Observer 3 | 0.03 | −0.07 to 0.13 | 1.0 |
| **Torsion (°)** |  |  |  |
| Observer 1 | 0.98 | 0.34 to 1.66 | 0.7 |
| Observer 2 | 1.02 | −0.65 to 2.65 | 0.1 |
| Observer 3 | 0.93 | −0.44 to 2.24 | 0.6 |
| **Axis (°)** |  |  |  |
| Observer 1 | 0.15 | −0.17 to 0.57 | 0.6 |
| Observer 2 | 0.17 | 0.01 to 0.33 | 0.2 |
| Observer 3 | 0.23 | −0.18 to 0.64 | 0.2 |

*MAD* Mean absolute difference, *95% CI* 95% confidence interval
[a]Statistical signficance of a one-sample *t*-test

for length measurement of phantom 1 was 0.03 mm, for torsion measurement of phantom 2 (femur) 0.98°, and for axis measurement of phantom 2 (tibia) 0.18°.

Clinical application

There was a significant ($P<0.001$) underestimation of leg length with MR imaging (Table 4) as compared with long radiographs. The mean underestimation was −2.8±0.7% (2.4±0.5 cm) for all patients. Separating the patient groups into genu varum and genu valgum showed significant underestimation with MRI in both groups (Table 4). The HKA angle of all patients, including varus and valgus knees, was slightly underestimated with MRI (Table 4). Separating the patient groups into genu varum and genu valgum led to a nonsignificant underestimation of the HKA angle with MRI of −0.5±1.0° (5.0±24.1%; $P=0.08$) in the

**Table 2** Interobserver reproducibility of length analysis of the acrylic glass phantom (phantom 1), torsion analysis of the femur phantom (phantom 2), and anatomical axis analysis of the tibia phantom (phantom 2)

|  | MAD | 95% CI |
|---|---|---|
| Length (mm) | 0.04 | −0.08 to 0.16 |
| Torsion (°) | 1.31 | −0.26 to 2.88 |
| Axis (°) | 0.22 | −0.21 to 0.65 |

*MAD* Mean absolute difference, *95% CI* 95% confidence interval

**Table 3** Accuracy of length analysis of the acrylic glass phantom (phantom 1), torsion analysis of the femur phantom (phantom 2) and anatomical axis analysis of the tibia phantom (phantom 2) based on comparison of MRI measurements and physical measurements with micrometer screw and goniometer

|  | MAD | 95% CI |
|---|---|---|
| Length (mm) | 0.03 | −0.07 to 0.13 |
| Torsion (°) | 0.98 | −0.24 to 2.20 |
| Axis (°) | 0.18 | −0.13 to 0.49 |

*MAD* Mean absolute difference, *95% CI* 95% confidence interval

varus knees (Fig. 4), whereas there was a significant underestimation of −3.6±2.8° (128±129%; $P=0.02$) in the valgus knees (Table 4, Fig. 5).

## Discussion

In this study, we have optimized and applied an MRI-based technique to analyze complex leg geometry. In a phantom study, we showed that this MR technique allows a highly accurate and reproducible determination of length, torsion, and axis. In the patient study, on the other hand, a significant underestimation of leg length was found compared to long radiographs, both in varus and valgus knees. As far as leg alignment determination is concerned, no relevant difference was found in varus knees comparing MRI and full load-bearing long radiographs in bipedal stance. In valgus knees, on the other hand, the MRI technique led to a significant underestimation of the extent of valgus malalignment.

Long radiographs are still the standard of reference for planning corrective surgery [3]. However, they have the problem of radiation exposure. Furthermore long radiographs are not reliable if the patella is rotated more than 10° off the frontal plane [19], and they show more severe development of valgus angulations with knee flexion compared to full extension [20], which is quite common, especially in patients with severe deformities of the lower extremity. Alternative methods for quantification of limb length discrepancies and rotation deformities are CT and ultrasound examinations [4–6]. CT provides the best assessment of osseous structures [21] but is again very limited by the disadvantage of radiation exposure. Ultrasound, on the other hand, cannot offer the high accuracy obtained by radiographic methods [5, 8].

MRI represents the most accurate imaging modality for evaluating soft-tissue and cartilage [19], making it the standard of reference, especially for the diagnosis of knee injuries. When applying MRI, no radiation exposure is required. However, until now, MRI measurements have only been introduced into the diagnosis of leg deformities for femoral anteversion in pediatric patients with femoral

**Table 4** Differences in leg length measurement and HKA angle measurement between long radiographs (upright position) and the MRI technique (supine position) in patients with genu varum and genu valgum

|  | Leg length (cm) | | | HKA (°) | | |
|---|---|---|---|---|---|---|
|  | LR | MRI | Difference[a] (%) | LR | MRI | Difference[a] (%) |
| Total | 85.1±6.0 | 83.1±6.0 | −2.8±0.7* | 3.7±8.8 | 4.2±7.2 | −32.6±82.0 |
| Genu varum | 83.5±5.6 | 81.4±5.4 | −3.0±0.4* | 8.2±4.9 | 7.6±4.4 | −5.0±24.1 |
| Genu valgum | 87.0±5.6 | 85.2±6.0 | −2.6±1.1* | −8.5±2.4 | −4.9±2.9 | −127.6±128.6* |

Data are presented as mean values ± standard deviation

*LR* Long radiograph, *MRI* magnetic resonance imaging

*$P<0.05$

[a]Difference represents overestimation (+) or underestimation (−) of leg length or HKA by MRI in percent

rotation osteotomies [11] and growth-plate changes in tibia vara prior to oblique osteotomy or tibial hemiepiphysiodesis [12]. These applications are based on axial MRI images at the center of the main magnetic field and, hence, the gradient fields used for image reconstruction. Therefore, spatial distortions at the borders of the FoV have minor or no impact on measurement results.

On the other hand, long-range measurements across the entire FoV will certainly produce an underestimation of acquired distances, since the gradients in the three imaging planes lose strength at the imaging margins. The scanned object seems to be "shrunk" and measurements at the imaging margins will present too short distances in all three planes. In the comparative study by Leitzes et al. [10], this effect was shown on cadaveric femurs at an FoV of 460–480 mm, producing a mean absolute difference of −2.9 mm as compared to gross caliper measurements. To our knowledge, this has been the one single publication that investigated possible length measurement differences comparing radiography, CT, and MRI.

In our phantom study, we were able to show that the effects of spatial distortions generated by gradient field inhomogeneities at the imaging borders can be completely avoided. This was done by using the largest possible FoV (400 mm) in the frequency encoding direction and halving the FoV in the phase encoding direction, i.e., z-direction acquiring coronal images. Therefore, each single coronal image produced data of exactly 200 mm in length in the z-axis. To eliminate wraparound artifacts, 100% phase oversampling was utilized. Five consecutive table positions without gap or overlap in the z-direction covered 1,000-mm leg length, which was sufficient to evaluate our patients. Longer legs necessitate a further imaging position. Applying this technique excluded errors induced by spatial distortions due to field inhomogeneities and produced accurate and reproducible measurements across long distances, as compared to gross length measurements.

To ensure true coronal imaging, the lower limb was supported with cushions and pads of increasing thickness from the knees to the ankles. Patient movement was minimized by fixing straps. Additionally, the image acquisition time was kept as short as possible. This was done by using the maximum gradient strengths in all three imaging planes and an increased bandwidth (500 Hz/pixel). With this, TE and TR were shortened to a minimum while supplying the needed number of slices (this might easily be reduced further), and the imaging time for the entire leg length was 125 s. The resulting intermediate contrast weighting was useful for this investigation, since anatomical details were accurately displayed. The increased bandwidth created the additional advantage of minimized chemical shift artifacts. This is important to accurately delineate cortical bone in an area containing lipids (yellow bone marrow).

In contrast to Leitzes et al. [10], we did not use any surface coils. The application of a surface coil for the investigation of a cadaveric femur at one imaging position is useful to increase the signal-to-noise ratio. This would have been valuable for a patient study as well, since imaging time could have been reduced further. On the other hand, in a patient study both legs would have to be covered completely with surface coils, which is possible with existing coil array systems of recent MR scanners. But the time for correct positioning of the patients' legs to obtain true coronal images would markedly increase. Since the signal-to-noise ratio in our images (Figs. 4 and 5) was sufficient to perform measurements, we preferred to acquire the images with the built-in body coil of the scanner.

The TSE sequence was selected for two reasons. First, in comparison with SE sequences, the signal that is collectable in a certain amount of time with given weighting and slice numbers is higher. Second, for anatomical imaging, TSE sequences are preferable in comparison with other sequence types since the sensitivity for susceptibility artifacts that arise at bone-soft tissue borders is very low. Therefore, cortical bone will be visualized as accurately as possible. In contrast, gradient echo sequences are very sensitive for field inhomogeneities and other artifacts. The intermediate, somewhat T1-

weighted imaging resulted from the minimized TE and TR, which was done to increase image acquisition speed.

In our phantom study we were able to show that MRI offers a highly reproducible and accurate tool for the measurement of length, torsion, and axis, independent of field of view limitations and magnetic field inhomogeneities. The analysis of the MADs revealed that intra- and interobserver reproducibilities were smaller as compared with the studies of Leitzes et al. [10], Sabharwal et al. [22], and Terry et al. [23]. These authors measured limb length with MRI scanogram, CT scanogram [10], full-length standing radiographs [22], and clinically [23] and compared their data with supine radiographic scanograms [10, 22, 23]. They also calculated intraclass correlation coefficients (ICC). That was not possible in our setting, since the gold standard in our phantom studies was mechanical measurement with high-precision instruments. The ICC can only be calculated if the intraobserver variation (and also the variation within the gold-standard measurements) is greater than zero, which is not the case in our study.

In applying the described technique to patients in the given setting with genu varum and genu valgum, we focused on the determination of leg length and leg axis. Again we could show high accuracy for our MR technique. Due to the fact that any cross-sectional MRI-based measurements are not hampered by projectional length distortion as in radiography, it was expected that long radiographs would overestimate the length of the leg when compared to MRI. According to the intercept theorem, a given true leg length of 80 cm will be displayed as 83.4 cm on radiographs with a film-to-focus distance of 250 cm and an estimated distance from the femoral head and the ankle joint to the film of 15 and 5 cm, respectively. That represents an overestimation with long radiographs of 4.3%. The overestimation of the radiographs compared to MRI measurements described herein was lower than expected. Although it is known that radiographs obtained with the patient standing and those obtained with the patient supine reveal high level correlation regarding leg length [24], the severe deformities in our patients might explain the slight deviation.

Regarding limb axis we could furthermore show that the effect of full weight bearing was not relevant for the diagnosis of varus malalignment. We saw an underestimation of only $0.5 \pm 1.0°$ with the MRI technique. That is in good agreement with the findings of Brouwer et al. [25] showing an average of only 2° less varus deviation in the supine position than in the standing position using radiographs.

Basically, the accuracy of in-plane measurements in every acquired image corresponds to the pixel size. The image resolution is virtually enhanced by interpolation of all visualization systems (e.g., monitor, digital laser print). Therefore, the displayed measurement accuracy as given by all software tools in clinical practice is higher than the acquired pixel resolution. This basic principle has to be kept in mind for the analysis of the accuracy of every image-based measurement in medicine.

The fact that valgus malalignment was not registered as accurately as varus malalignment by the new MRI technique shows one limitation of this method. These findings support the concept of increased ligament stiffness in varus osteoarthritis [26] and the well-known weakening of the medial knee joint stabilizers in valgus malalignment [27]. So some deformities that depend not only on the bones but also on the joint stability and cartilage morphology can probably not be assessed correctly without simulation of the body weight [28, 29]. In the future this limitation should be solved with an MRI-compatible weight-bearing apparatus. However, in posttraumatic or hereditary deformities, the problem is mostly restricted to the bones [3], which can be assessed very accurately with our new MR technique. As we showed with our phantom study, the presented MRI technique can accurately determine length, axis, and torsion of a solid body. However, due to concerns regarding metal artifacts, MRI shows limited applicability for the planning and control of corrective surgery as long as metal implants are in situ.

Applying the presented MRI technique, reproducible and accurate data from patients in supine position on leg length, axis and torsion are available. The only method that provides comparable data is CT, including a scanogram and axial scans. The acquisition time for both methods is approximately the same, 4–5 min. Besides the lack of radiation exposure, MRI has the advantage that further information on the soft-tissue structures, especially the knees, would be available in the same session.

In conclusion, this paper shows that the presented MRI technique offers a highly accurate tool for the measurement of length, torsion, and axis, as shown in the phantom study. Selecting optimized MRI techniques excludes spatial distortions that might hamper measurements or image fusion that occurs with other modalities. In the patient study, varus deformities were registered accurately, while in valgus knees, a significant difference in leg length and leg axis compared to long radiographs was found. This effect is caused, on one hand, by the projectional inaccuracy of conventional radiography, and, on the other hand, even more by the effect of different assessment positions. So, the influence of body mass is more pronounced in loose valgus knees than in tight varus knees.

This radiation-free technique can be used for an accurate analysis of lower limb deformities and thus for improved planning prior to corrective surgery if the deformities are limited to the bones. If an additional effect of joint instability is relevant for axis deformity, the technique needs to be improved by simulating the influence of body weight.

# References

1. Paley D, Tetsworth K (1992) Mechanical axis deviation of the lower limbs. Preoperative planning of uniapical angular deformities of the tibia or femur. Clin Orthop 280:48–64
2. Paley D, Tetsworth K (1992) Mechanical axis deviation of the lower limbs. Preoperative planning of multiapical frontal plane angular and bowing deformities of the femur and tibia. Clin Orthop 280:65–71
3. Paley D, Herzenberg JE, Tetsworth K, McKie J, Bhave A (1994) Deformity planning for frontal and sagittal plane corrective osteotomies. Orthop Clin North Am 25:425–465
4. Keppler P, Strecker W, Kinzl L (1999) CT determination of leg length and torsion in children and adolescents. Unfallchirurg 102:936–941
5. Keppler P, Strecker W, Kinzl L, Simmnacher M, Claes L (1999) Sonographic imaging of leg geometry. Orthopade 28:1015–1022
6. Strecker W, Keppler P, Gebhard F, Kinzl L (1997) Length and torsion of the lower limb. J Bone Joint Surg Br 79:1019–1023
7. Kalra MK, Maher MM, Toth TL et al (2004) Strategies for CT radiation dose optimization. Radiology 230:619–628
8. Terjesen T, Benum P, Rossvoll I, Svenningsen S, Floystad Isern AE, Nordbo T (1991) Leg-length discrepancy measured by ultrasonography. Acta Orthop Scand 62:121–124
9. van der Schoot DK, Den Outer AJ, Bode PJ, Obermann WR, van Vugt AB (1996) Degenerative changes at the knee and ankle related to malunion of tibial fractures. 15-year follow-up of 88 patients. J Bone Joint Surg Br 78:722–725
10. Leitzes AH, Potter HG, Amaral T, Marx RG, Lyman S, Widmann RF (2005) Reliability and accuracy of MRI scanogram in the evaluation of limb length discrepancy. J Pediatr Orthop 25:747–749
11. Tomczak RJ, Guenther KP, Rieber A, Mergo P, Ros PR, Brambs HJ (1997) MR imaging measurement of the femoral antetorsional angle as a new technique: comparison with CT in children and adults. AJR Am J Roentgenol 168:791–794
12. Synder M, Vera J, Harcke HT, Bowen JR (2003) Magnetic resonance imaging of the growth plate in late-onset tibia vara. Int Orthop 27:217–222
13. Aamodt A, Terjesen T, Eine J, Kvistad KA (1995) Femoral anteversion measured by ultrasound and CT: a comparative study. Skelet Radiol 24:105–109
14. Keats TE, Teeslink R, Diamond AE, Williams JH (1966) Normal axial relationships of the major joints. Radiology 87:904–907
15. Hsu RWW, Himeno S, Coventry MB, Chao EYS (1990) Normal axial alignment of the lower extremity and load bearing distribution at the knee. Clin Orthop Rel Research 255:215–227
16. Bland JM, Altman DG (1995) Comparing methods of measurement: why plotting difference against standard method is misleading. Lancet 346:1085–1087
17. Bland JM, Altman DG (1990) A note on the use of the intraclass correlation coefficient in the evaluation of agreement between two methods of measurement. Comput Biol Med 20:337–340
18. Bland JM, Altman DG (1986) Statistical methods for assessing agreement between two methods of clinical measurement. Lancet 1:307–310
19. Wright JG, Treble N, Feinstein AR (1991) Measurement of lower limb alignment using long radiographs. J Bone Joint Surg Br 73:721–723
20. Koshino T, Takeyama M, Jiang LS, Yoshida T, Saito T (2002) Underestimation of varus angulation in knees with flexion deformity. Knee 9:275–279
21. Lang P, Genant HK, Jergesen HE, Murray WR (1992) Imaging of the hip joint. Computed tomography versus magnetic resonance imaging. Clin Orthop 274:135–153
22. Sabharwal S, Zhao C, McKeon J, Melaghari T, Blacksin M, Wenekor C (2007) Reliability analysis for radiographic measurement of limb length discrepancy: full-length standing anteroposterior radiograph versus scanogram. J Pediatr Orthop 27:46–50
23. Terry MA, Winell JJ, Green DW, Schneider R, Peterson M, Marx RG, Widmann RF (2005) Measurement variance in limb length discrepancy: clinical and radiographic assessment of interobserver and intraobserver variability. J Pediatr Orthop 25:197–201
24. Cleveland RH, Kushner DC, Ogden MC, Herman TE, Kermond W, Correia JA (1988) Determination of leg length discrepancy. A comparison of weight-bearing and supine imaging. Invest Radiol 23:301–304
25. Brouwer RW, Jakma TS, Bierma-Zeinstra SM, Ginai AZ, Verhaar JA (2003) The whole leg radiograph: standing versus supine for determining axial alignment. Acta Orthop Scand 74:565–568
26. Fishkin Z, Miller D, Ritter C, Ziv I (2002) Changes in human knee ligament stiffness secondary to osteoarthritis. J Orthop Res 20:204–207
27. Markolf KL, Mensch JS, Amstutz HC (1976) Stiffness and laxity of the knee - the contributions of the supporting structures. A quantitative in vitro study. J Bone Joint Surg Am 58:583–594
28. Saeki K, Mihalko WM, Patel V et al (2001) Stability after medial collateral ligament release in total knee arthroplasty. Clin Orthop 392:184–189
29. Patel VV, Hall K, Ries M, Lotz J, Ozhinsky E, Lindsey C, Lu Y, Majumdar S (2004) A three-dimensional MRI analysis of knee kinematics. J Orthop Res 22:283–292